Title

Cortical Bone Loss Following Gastric Bypass Surgery Is Not Primarily Endocortical

Journal

Journal of Bone and Mineral Research, 37(4)

ISSN

0884-0431

Authors

Sadoughi, Saghi

Pasco, Courtney

Joseph, Gabby B

et al.

Publication Date

2020-12-01

DOI

10.1002/jbmr.4512

Peer reviewed

HHS Public Access

Author manuscript

J Bone Miner Res. Author manuscript; available in PMC 2022 July 01.

Published in final edited form as:

J Bone Miner Res. 2022 April ; 37(4): 753–763. doi:10.1002/jbmr.4512.

Cortical Bone Loss Following Gastric Bypass Surgery Is Not Primarily Endocortical

Saghi Sadoughi[1], **Courtney Pasco**[1], **Gabby B Joseph**[1], **Po-Hung Wu**[1], **Anne L Schafer**[2,3,4], **Galateia J Kazakia**[1]

[1]Musculoskeletal Quantitative Imaging Research Group, Department of Radiology and Biomedical Imaging, University of California, San Francisco, CA, USA

[2]Department of Medicine, University of California, San Francisco, CA, USA

[3]Endocrine Research Unit, San Francisco VA Health Care System, San Francisco, CA, USA

[4]Department of Epidemiology and Biostatistics, University of California, San Francisco, CA, USA

Abstract

Roux-en Y gastric bypass (RYGB) surgery is an effective treatment for obesity; however, it may negatively impact skeletal health by increasing fracture risk. This increase may be the result not only of decreased bone mineral density but also of changes in bone microstructure, for example, increased cortical porosity. Increased tibial and radial cortical porosity of patients undergoing RYGB surgery has been observed as early as 6 months postoperatively; however, local microstructural changes and associated biological mechanisms driving this increase remain unclear. To provide insight, we studied the spatial distribution of cortical porosity in 42 women and men (aged 46 ± 12 years) after RYGB surgery. Distal tibias and radii were evaluated with high-resolution peripheral quantitative computed tomography (HR-pQCT) preoperatively and at 12 months postoperatively. Laminar analysis was used to determine cortical pore number and size within the endosteal, midcortical, and periosteal layers of the cortex. Paired *t* tests were used to compare baseline versus follow-up porosity parameters in each layer. Mixed models were used to compare longitudinal changes in laminar analysis outcomes between layers. We found that the midcortical (0.927 ± 0.607 mm^{-2} to 1.069 ± 0.654 mm^{-2}, $p = 0.004$; 0.439 ± 0.293 mm^{-2} to 0.509 ± 0.343 mm^{-2}, $p = 0.03$) and periosteal (0.642 ± 0.412 mm^{-2} to 0.843 ± 0.452 mm^{-2}, $p < 0.0001$; 0.171 ± 0.101 mm^{-2} to 0.230 ± 0.160 mm^{-2}, $p = 0.003$) layers underwent the greatest increases in porosity over the 12-month period at the distal tibia and radius, respectively. The endosteal layer, which had the greatest porosity at baseline, did not undergo significant porosity increase

Address correspondence to: Saghi Sadoughi, PhD, Department of Radiology and Biomedical Imaging, 185 Berry Street, Lobby 6, Suite 350, San Francisco, CA 94107, USA. saghi.sadoughi@ucsf.edu.

Author Contributions

Saghi Sadoughi: Conceptualization; formal analysis; investigation; methodology; software; visualization; writing – original draft; writing – review and editing. **Courtney Pasco:** Conceptualization; investigation; methodology; software; writing – review and editing. **Gabby B Joseph:** Formal analysis; writing – review and editing. **Po-Hung Wu:** Conceptualization; methodology; software; writing – review and editing. **Anne Louise Schafer:** Conceptualization; funding acquisition; project administration; resources; supervision; writing – review and editing. **Galateia J Kazakia:** Conceptualization; funding acquisition; methodology; project administration; resources; supervision; visualization; writing – review and editing.

Disclosures

ALS receives research support from Amgen (investigator-initiated grant) and Bariatric Advantage (supplements donated for study). All other authors state that they have no conflicts of interest.

over the same period (1.234 ± 0.402 mm^{-2} to 1.259 ± 0.413 mm^{-2}, $p = 0.49$; 0.584 ± 0.290 mm^{-2} to 0.620 ± 0.299 mm^{-2}, $p = 0.35$) at the distal tibia and radius, respectively. An alternative baseline-mapping approach for endosteal boundary definition confirmed that cortical bone loss was not primarily endosteal. These findings indicate that increases in cortical porosity happen in regions distant from the endosteal surface, suggesting that the underlying mechanism driving the increase in cortical porosity is not merely endosteal trabecularization. © 2022 American Society for Bone and Mineral Research (ASBMR).

Keywords

GASTRIC BYPASS SURGERY; HR-pQCT; BONE MICROSTRUCTURE; CORTICAL POROSITY; LAMINAR ANALYSIS

Introduction

Obesity, which is associated with significant morbidity and mortality,[1] is a critical public health issue. Although weight loss for obesity has been associated with improvement in comorbidities and reduced mortality,[2] nonoperative efforts for weight loss (eg, exercise, diet, other lifestyle changes) do not always guarantee a long-term resolution for morbidly obese individuals.[3] Even recent advances in pharmacologic therapy[4] are inadequate for weight loss of the magnitude required by many severely obese individuals. Bariatric surgery provides a more durable solution.[5,6] One commonly performed bariatric operation is Roux-en Y gastric bypass (RYGB). Although an effective treatment for obesity, previous studies suggest that RYGB surgery may negatively impact skeletal health by increasing bone turnover and decreasing bone mineral density (BMD).[7-13] Fracture risk is also elevated after RYGB,[14-19] with the increased risk of major osteoporotic fractures driven by a twofold risk of wrist, forearm, and hip fracture.[20] This increase in fracture risk may be the result not only of decreased BMD but also of changes in bone microstructure—for example, an increase in cortical porosity, as cortical porosity has recently been studied as a potential risk factor for fragility fractures.[21-24] Our group found an increase in the radial and tibial cortical porosity of patients undergoing RYGB surgery as early as 6 months postoperatively.[25] Yet, local microstructural changes and the underlying biological mechanisms that drive the increase in cortical porosity in individuals undergoing RYGB surgery remain unclear.

Multiple mechanisms of pore space expansion may drive the increased cortical porosity after an RYGB surgery. Potential mechanisms include marrow cavity expansion (trabecularization), vascular network expansion, perilacunarcanalicular resorption, and/or combinations of two or more mechanisms. Knowledge of the spatial distribution of new pore space within the cortex may help better determine where the porosity changes occur and, therefore, provide insight into the possible mechanisms driving these changes. Investigating the spatial distribution of the cortical pores also has mechanical importance because it is established that pores located closest to the periosteal surface have the most detrimental effects on mechanical properties.[26,27] To provide insight, here we sought to quantify the spatial distribution of cortical porosity in patients after RYGB surgery. More specifically, we did so by calculating cortical pore number and size in the endosteal, midcortical, and

periosteal layers of the cortex in the distal radius and distal tibia of patients preoperatively and at 12 months postoperatively. We hypothesized that the increase in cortical porosity after RYGB surgery would be due primarily to endocortical trabecularization. The knowledge provided by the results of this study may lead to the development of more targeted and therefore more effective therapeutics.

Materials and Methods

Study population

Women and men aged 25 to 70 years were recruited from two academic bariatric surgery centers (the University of California, San Francisco, and the San Francisco Veterans Affairs Health Care System). Inclusion and exclusion criteria have been described in detail previously[25] In short, participants were eligible if scheduled for an RYGB procedure. Perimenopausal women (defined as last menses >3 months but <5 years ago) were excluded. Premenopausal women on stable hormonal contraception, postmenopausal women on stable hormone therapy, and men on stable testosterone were eligible. Participants were excluded if they used medications known to impact bone and mineral metabolism, including antiresorptive or osteoanabolic bone-specific drugs (in the last year or for >12 months ever), oral glucocorticoids (>5 mg prednisone equivalent daily for >10 days in the last 3 months), and thiazolidinediones. Other exclusion criteria included prior bariatric surgery, weight >159 kg (the dual-energy X-ray absorptiometry [DXA] scanner weight limit), estimated glomerular filtration rate <30 mL/min/1.73 m^2, and diseases known to affect bone (eg, primary hyperparathyroidism, Paget's disease, or clinically significant liver disease). Patients with active malignant diseases were not eligible for surgery at the participating institutions and, thus, were not enrolled in the study.

Study protocol

The study protocol has been described in detail previously.[25] In brief, the protocol standardized calcium intake and vitamin D status. At enrollment, low 25(OH)D levels were repleted to a target level ≥30 ng/mL, and each participant's total daily calcium intake was brought to 1200 mg based on estimation of dietary intake.[28] Similarly, in the postoperative period, each participant's supplement doses were adjusted to maintain vitamin D and calcium intake goals. The RYGB procedure was performed in a standardized laparoscopic fashion at both bariatric surgery centers as described previously.[25] Participants were evaluated with DXA, quantitative computed tomography (QCT), and high-resolution peripheral quantitative computed tomography (HR-pQCT) preoperatively and at 6 and 12 months postoperatively as part of our earlier study.[25] Baseline and 12-month follow-up data were analyzed for the present study. Six of the original participants were excluded because neither radius nor tibia analysis yielded results for technical reasons (eg, poor longitudinal registration or very thin cortical bone).

The University of California, San Francisco, institutional review board approved the study protocol (#11-05870, original date of approval March 3, 2011), and all participants provided written informed consent. The study was registered at www.clinicaltrials.gov (NCT01330914).

DXA

Areal bone mineral density (aBMD, g/cm^2) of the proximal femur and lumbar spine (L_1 to L_4) was measured by DXA (Hologic Discovery Wi densitometer, Bedford, MA, USA) preoperatively and at 12 months postoperatively. The local coefficient of variation (CV) derived from the manufacturer phantom for spinal BMD is 0.437%.

QCT

Volumetric QCT of the L_3 and L_4 vertebrae was performed preoperatively and at 12 months postoperatively (General Electric VCT64 scanner, Milwaukee, WI, USA), as described in detail previously.[29] Trabecular volumetric BMD (vBMD, g/cm^3) was evaluated using QCTPro (Mindways Software, Inc., Austin, TX, USA), with one experienced operator evaluating all the scans. The root mean square coefficient of variation (RMSCV) for trabecular volumetric BMD is 1.7%.[30]

HR-pQCT

Acquisition—A first-generation HR-pQCT system (XtremeCT, Scanco Medical, Bruttisellen, Switzerland) was used to scan participants preoperatively and at 12 months postoperatively, using the manufacturer's standard in vivo protocol (source potential 60 kVp, tube current 900 mA, isotropic 82 μm nominal resolution).[31,32] The nondominant forearm and lower leg were scanned, with fixed scan region starting at 9.5 mm and 22.5 mm proximal to the joint for the distal radius and tibia, respectively, and extending 9.02 mm proximally (110 slices). The contralateral side was imaged if a history of fracture was reported on the nondominant side. RMSCV values are <1.4% for densitometric parameters, and 1.3% to 8.9% for structural parameters.[33]

All scans were visually inspected for motion artifacts using the manufacturer's grading scheme[34] to ensure all the images included in further analyses were of adequate quality (grades 1 to 3).

Cortical segmentation—Cortical bone compartment segmentation was performed using a customized image processing language (IPL v.506a-ucsf, Scanco Medical AG) by applying a semiautomated three-step image processing algorithm, as described in detail previously.[35] In short, first an auto-contouring process was used to identify the periosteal and endosteal cortical boundaries; these auto-contours were checked and corrected manually if necessary. Next, pores within the cortical compartment were identified. Finally, the cortical compartment mask and the pore mask were combined to create a final, refined mask of the cortical compartment.

Laminar analysis—Laminar analysis was performed using MATLAB (MathWorks, Inc., Natick, MA, USA). The segmented cortical compartment was sub-divided into three concentric layers corresponding to the endosteal, midcortical, and periosteal laminar layers as described in detail previously.[36,37] Then a skeletonization procedure was utilized to deconstruct the pore network into individual elements,[38] so that the location of each pore centroid could be determined. Based on the location of its centroid, each pore was assigned to a layer (Fig. 1). Three metrics were computed to characterize cortical porosity within each

layer: total pore area (TPA, mm^2/mm^2), total pore number (TPN, mm^{-2}), and average pore area (APA, mm^2). In each slice of the analyzed volume, TPA was calculated as the sum of all pore areas assigned to a specific layer. TPN was calculated as the total number of pores within each layer. Both TPA and TPN values were normalized by the area of each layer to prevent skewed results due to the larger area of periosteal versus endosteal layers. APA was calculated as the mean pore area within each layer. RMSCV for laminar analysis metrics ranged from 3.04% to 3.94% for the midcortical, from 4.37% to 6.09% for the periosteal, and from 5.77% to 9.35% for the endosteal layer.[37]

Baseline mapping

To confirm and support the conclusions drawn from our laminar analysis, we performed baseline mapping, which is a distinct but parallel approach for assessing longitudinal changes at the endosteal surface. This technique was employed to investigate the impact of endosteal cortical margin definition on porosity data. In this baseline mapping process, baseline and follow-up HR-pQCT data sets were automatically registered based on full 3D mutual information routines and only the volume common to both time points was analyzed. Longitudinal data were recalculated using an alternate endosteal boundary definition for the follow-up data set—the baseline endosteal boundary was mapped (transformed) onto the follow-up image using MATLAB (MathWorks, Inc., Fig. 2), as has been demonstrated on a number of data sets by our group and others.[39,40] This allowed us to eliminate the influence of redefining the endosteal contour at follow-up. Cortical thickness (Ct.Th, mm), cortical pore volume (Ct.Po.V, mm^3), cortical porosity (Ct.Po, unitless ratio), mean cortical pore diameter (Po.Dm, mm), and standard deviation of mean cortical pore diameter (Po.Dm.SD, mm) were the metrics evaluated. By comparing standard to baseline-mapped longitudinal porosity data, we evaluated the role of endocortical trabecularization on the calculation of porosity and pore distribution at the follow-up time point.

Other measures

Body mass index (BMI) was calculated as weight/height^2 (kg/m^2). Estimates of dietary intake were obtained using the Block food-frequency questionnaire.[41] Physical activity was assessed using the International Physical Activity Questionnaire (IPAQ) short form.[42] Serum samples were collected after an overnight fast for determination of hemoglobin A_{1c} (HbA_{1c}), 25(OH)D, and intact parathyroid hormone (PTH).

Statistical analysis

To determine whether baseline characteristics differed between groups, normality assessment was performed. For normally distributed characteristics (presented as means ± SDs), linear regression models were utilized. For characteristics with skewed distributions (presented as medians and interquartile ranges [IQR]), the nonparametric Kruskal–Wallis test was utilized. Next, paired *t* tests were used to compare baseline versus follow-up measurements for laminar analysis outcomes (ie, TPA, TPN, and APA) in each laminar layer and to compare longitudinal changes in porosity parameters (ie, Ct.Th, Ct.Po.V, Ct.Po, Po.Dm, Po.Dm.SD) calculated with standard versus baseline-mapping technique in the cortex. Mixed models (accounting for multiple measurements per participant) were used to compare the longitudinal changes in laminar analysis outcome measurements (ie, %change

in TPA, TPN, and APA) between laminar layers (endosteal, midcortical, periosteal). These models were stratified by sex and menopause status. Statistical analyses were performed using STATA 16 software (StataCorp, College Station, TX, USA) with significance set at $p < 0.05$.

Results

Baseline participant characteristics

A summary of the study population baseline characteristics is given in Table 1. Of the 42 participants, 9 (21%) were men, 23 (55%) were premenopausal women, and 10 (24%) were postmenopausal women. Three postmenopausal women were on stable hormone replacement therapy, and two men were on stable testosterone replacement. Two men and one premenopausal and one postmenopausal woman were using proton-pump inhibitors. Participants were aged 46 ± 12 (mean ± SD) years overall; on average, premenopausal women were younger than postmenopausal women and men. Postmenopausal women had lower weight than men; however, BMI did not differ by sex or menopausal status.

Vitamin D status and PTH, cholesterol, and triglyceride levels did not differ by sex or menopausal status. Premenopausal women had lower HbA_{1c} levels than postmenopausal women and men. Physical activity and dietary protein did not differ by sex or menopausal status.

Postmenopausal women had lower aBMD at the femoral neck than premenopausal women. Total hip and lumbar spine aBMD did not differ by sex or menopausal status. Postmenopausal women had lower spinal vBMD than premenopausal women.

The participants in this study were a subset of a cohort described in a previous publication.[25] Six of the original participants were excluded because neither radius nor tibia analysis yielded results for technical reasons (eg, poor longitudinal registration or very thin cortical bone). Of the remaining 42 participants, a subset of 37 contributed data for the distal tibia; the remainder had to be excluded for technical reasons. A slightly different subset of 37 contributed data for the distal radius.

Longitudinal changes in weight and axial BMD

Across all the participants, overall weight decreased by 30.46 ± 7.07% at the 12-month follow-uptime point ($p < 0.0001$). As previously reported for the complete cohort,[25] total hip and femoral neck areal BMD decreased 12 months after the surgery. The decreases were by 8.45 ± 5.22% ($p < 0.0001$) at the total hip and by 8.05 ± 4.92% ($p < 0.0001$) at the femoral neck. As previously reported,[25] lumbar spine areal BMD showed a slight but insignificant decrease over 12 months (by 1.33 ± 5.23%, $p = 0.08$), whereas spine volumetric BMD decreased significantly (by 8.07 ± 6.83%, $p < 0.0001$).

All premenopausal women had normal bone mass at baseline and follow-up, with normal bone mass defined here as Z-score > −1.0. Among postmenopausal women, two had osteopenia at baseline, defined as T-score of −1.0 to −2.4; both were still in the osteopenia range at follow-up. Three postmenopausal women had normal bone mass at baseline, then

developed osteopenia at follow-up. Among men 50 years of age or older, using *T*-scores, one man had osteopenia at baseline and follow-up. Among men younger than 50 years, one had normal bone mass at baseline, then developed osteopenia at follow-up, defined here as *Z*-score ≤ −1.0.

Longitudinal changes in overall porosity parameters

As previously reported for the complete cohort,[25] cortical porosity, cortical pore volume, and cortical pore diameter increased at the 12-month postoperative time point by 16.05 ± 18.01% ($p < 0.0001$), 16.95 ± 26.39% ($p = 0.001$), and 6.06 ± 8.71% ($p = 0.0004$), respectively, at the distal tibia. At the distal radius, cortical porosity and cortical pore diameter increased by 12.88 ± 32.52% ($p = 0.02$) and 3.87 ± 9.77% ($p = 0.03$), respectively, at the 12-month postoperative time point; cortical pore volume, however, showed an insignificant increase of 10.32 ± 32.64% ($p = 0.06$). As previously reported,[25] cortical thickness decreased at the 12-month postoperative time point by 3.41 ± 4.42% ($p < 0.0001$) at the distal tibia and by 2.94 ± 4.53% ($p = 0.0001$) at the distal radius.

Baseline spatial pore distribution

At baseline at the distal tibia, TPA and TPN were the highest in the endosteal and the lowest in the periosteal layer across all the participants, whereas the midcortical value was in between the other two layers (Table 2). For APA, the lowest value was also observed in the periosteal layer; however, the midcortical layer had a marginally higher APA than the endosteal (Table 2). Statistically, TPA, TPN, and APA were significantly different across all layers ($p < 0.05$, $p < 0.0001$, and $p < 0.05$, respectively).

At the distal radius, TPA and TPN followed the same trend as in the distal tibia—both were the highest in the endosteal layer and the lowest in the periosteal layer across all the participants (Table 3). For APA, however, the lowest value was observed in the endosteal, followed by periosteal and midcortical layers (Table 3). Statistically, TPA in the endosteal and midcortical layers were both significantly higher than that in the periosteal layer (p) < 0.0001); however, endosteal and midcortical TPA were not significantly different from each other ($p = 0.08$). TPN and APA were significantly different across all layers (p) < 0.05).

Twelve-month spatial pore distribution

At the 12-month follow-up time point at the distal tibia, TPA and TPN still were the highest in the endosteal layer and the lowest in the periosteal layer across all the participants (Table 2). APA was the highest in the midcortical layer, whereas the lowest value was observed in the periosteal layer (Table 2). Statistically, TPA in the endosteal and midcortical layers were both significantly higher than that of the periosteal layer ($p < 0.0001$); however, endosteal and midcortical TPA were not significantly different from each other ($p = 0.99$). TPN was significantly different across all layers ($p < 0.05$). APA in the endosteal layer was significantly lower than in the midcortical layer ($p < 0.0001$) but not different from the periosteal layer ($p = 0.22$); midcortical layer also had a significantly higher APA than the periosteal layer ($p < 0.0001$).

At the distal radius, TPA and TPN were the highest in the endosteal layer and the lowest in the periosteal layer across all the participants 12 months postoperatively (Table 3). For APA, however, the lowest value was observed in the endosteal, followed by periosteal and midcortical layers (Table 3). Statistically, TPA in the endosteal and midcortical layers were both significantly higher than of the periosteal layer ($p < 0.0001$); however, endosteal and midcortical TPA were not significantly different from each other ($p = 0.73$). TPN and APA were significantly different across all layers ($p < 0.05$).

Longitudinal changes in spatial pore distribution

At the distal tibia, over the 12-month study period, TPA, TPN, and APA did not change significantly in the endosteal layer ($p > 0.1$ for all outcomes). However, TPA increased by 37.82 ± 47.16% (p 0.0001) and 58.77 ± 64.55% ($p < 0.0001$); TPN increased by 22.44 ± 33.02% ($p = 0.004$) and 43.78 ± 49.59% ($p < 0.0001$); and APA increased by 11.08 ± 15.03% ($p = 0.0002$) and 9.33 ± 11.10% ($p < 0.0001$) in the midcortical and periosteal layers, respectively (Table 2).

At the distal radius, over the 12-month study period, only TPN in the midcortical (21.28 ± 44.01%, $p = 0.03$) and periosteal (32.24 ± 55.60%, $p = 0.003$) layers increased significantly (Table 3).

Sex and menopause stratification

Stratifying the longitudinal changes in TPA, TPN, and APA at the distal tibia based on participants' sex and menopause status, we found that the greatest mean %changes occurred in postmenopausal women except for APA in the endosteal layer, which showed the greatest %change in men. In men, none of those relatively small longitudinal changes were statistically significant except for APA in the periosteal layer ($p = 0.01$ for baseline versus follow-up; Fig. 3). In premenopausal and postmenopausal women, TPA, TPN, and APA longitudinal changes were significant in the midcortical and periosteal layers ($p < 0.05$; Fig. 3).

Between-layer comparisons yielded significant differences in some of the longitudinal changes (Fig. 3). In men, mean % change in TPA and TPN in the endosteal layer were significantly smaller than those of the periosteal layer ($p = 0.002$ and $p = 0.001$, respectively); TPN %change in the midcortical layer was also smaller than that of the periosteal layer ($p = 0.01$). In premenopausal women, TPA, TPN, and APA %change in the endosteal layer were smaller than periosteal layer ($p < 0.0001$, $p < 0.0001$, and $p = 0.005$, respectively); TPA and APA %change in the endosteal layer were also smaller than the midcortical layer ($p = 0.01$ and $p < 0.0001$, respectively); TPA and TPN % change in the midcortical layer was smaller than the periosteal layer ($p = 0.001$ and $p < 0.0001$, respectively). In postmenopausal women, TPA, TPN, and APA %change in the endosteal layer were smaller than midcortical ($p = 0.003$, $p = 0.002$, and $p = 0.004$, respectively) and periosteal ($p = 0.006$, $p = 0.006$, and $p = 0.01$, respectively) layers; however, the latter two layers did not differ significantly in postmenopausal women.

Similarly, at the distal radius, the greatest mean percent changes occurred in postmenopausal women except for APA in the periosteal layer, which showed the greatest %change in

premenopausal women. In men and premenopausal women, none of the longitudinal changes were statistically significant ($p > 0.1$ for baseline versus follow-up; Fig. 4). In postmenopausal women, longitudinal changes in TPA in the periosteal ($p = 0.02$) and TPN in the midcortical ($p = 0.05$) and periosteal ($p = 0.005$) layers were statistically significant (Fig. 4).

Between-layer comparisons at the distal radius, however, yielded significant differences for fewer longitudinal changes compared with the distal tibia (Fig. 4). In men, mean %change in APA in the endosteal layer was significantly smaller than that of the midcortical and periosteal layers ($p = 0.03$ and $p = 0.001$, respectively). In premenopausal women, only TPN % change in the endosteal layer was smaller than the periosteal layer ($p = 0.04$). In postmenopausal women, TPN %change in the endosteal layer was smaller than that of the periosteal layer ($p = 0.04$).

Baseline mapping

To confirm the findings of our laminar analysis indicating that longitudinal changes in spatial pore distribution are not primarily endocortical, we employed the baseline mapping technique, which is a distinct but parallel approach for investigating longitudinal changes at the endosteal surface. Longitudinal changes in cortical porosity parameters calculated using standard approach were compared against longitudinal changes calculated using the baseline-mapping technique. The baseline-mapping technique maps the endosteal contour from the baseline to the follow-up data set, ensuring that the same endosteal border is evaluated at baseline and follow-up. We found no differences in longitudinal %change in porosity parameters calculated by the two techniques (Tables 4 and 5). This distinct approach confirms that longitudinal changes in porosity occur mostly in the midcortical and periosteal layers and not because of trabecularization of the endosteal surface. If longitudinal changes in porosity were primarily due to endosteal trabecularization, the baseline mapping approach would not yield equivalent longitudinal changes in porosity, but rather would capture increased porosity at the most endosteal aspect of the cortical compartment.

Discussion

The overall goal of this study was to assess the spatial pore distribution in the radial and tibial cortex of patients undergoing Roux-en Y gastric bypass surgery. We found that in our cohort, although the endosteal layer had the greatest pore number and pore area at both sites initially, the midcortical and periosteal layers underwent the greatest increases in porosity over time. The relatively small endocortical pore expansion makes it less likely for the increased porosity to be merely driven by trabecularization of the endosteal border of the cortical compartment. These findings indicate that increases in cortical porosity happen in regions other than the endosteal surface, suggesting that contrary to our hypothesis, the underlying mechanism driving the increase in cortical porosity is not merely endosteal trabecularization.

In contrast to these findings in a bariatric surgery cohort, we previously reported that a period of disuse resulted in a uniform increase in tibial cortical porosity throughout the cortex.[43] In a study of postmenopausal bone loss, we reported increased cortical

porosity concentrated within the endosteal cortex.[44] In a cross-sectional study of spatial pore distribution in the tibial cortex throughout the life span, we reported that age-related increases in porosity are most extreme in the midcortical layer.[37] Similarly, cortical laminar analysis in a type 2 diabetic postmenopausal cohort revealed increased porosity primarily in the midcortical layer at both radius and tibia in fracture group compared with the non-fracture group.[45] These previous studies together with the present study suggest that a single mechanism to drive the increase in cortical porosity may not exist and that different mechanisms may be in play in different cohorts and in different disease states.

In our cohort, the largest longitudinal increases in porosity were observed in the midcortical and periosteal layers. Given that midcortical and periosteal layers are highly susceptible, so-called watershed zones of the cortex,[46,47] one potential explanation could be that the increased porosity in those two layers may be driven by changes in cortical vascularization, for example, angiogenesis into the cortical space, possibly as a response to hypoxia in midcortical regions. However, further histological studies are required to better elucidate biological mechanisms driving these changes.

Our findings also yield insights about fragility fracture risk, as pores located close to the periosteal surface have more detrimental effects on mechanical properties.[26,27] Pores amplify local stress profiles and create stress concentrations that may facilitate the initiation and propagation of microcracks through bone tissue.[48,49] Pores located near the periosteal surface, the site of maximum stress under bending loads,[50] superimpose high local stress profiles over high bending stress. Therefore, the longitudinal increases in porosity observed preferentially in the mid-cortical and periosteal regions in this study could increase the risk of fragility fractures in patients undergoing RYGB. Similar to our findings, a previous study in our group found a higher porosity in the midcortical and periosteal layers in radius and tibia cortex of participants with history of fragility fractures compared with the participants without history of fragility fractures in postmenopausal women with type 2 diabetes.[45] Together these results suggest that it may be more effective for therapeutic efforts to focus on mechanisms that play a larger role in increasing the porosity of the midcortical and periosteal layers rather than the endosteal layer.

The main novelty of our study lies in its detailed nature of the pore distribution analysis while accounting for the possible biases in endosteal boundary identification. Our technique, developed in-house, made it possible to quantify the number and area of every pore in each of the three defined cortical layers. As a result, it was possible to track longitudinal changes of each region separately to provide insight relevant to biological mechanisms. It is true that the significant decrease observed in cortical thickness at the 12-month follow-up time point results in each layer being slightly narrower at follow-up compared with baseline; this is inherent to our laminar analysis technique and is the reason why we also employed our baseline mapping technique. We found similar longitudinal %change in porosity parameters using the two techniques (Tables 4 and 5). This confirms that the longitudinal increases in porosity in this cohort are not simply occurring at the endosteal surface through a process of trabecularization[51] and confirms that redefining the endosteal contour at the follow-up time point—as opposed to mapping the baseline contour—does not introduce biases by under- or overestimating the porosity changes and, therefore, supports the validity of our approach.

A number of limitations should be considered when interpreting our results. First, our scans were acquired using HR-pQCT. Although HR-pQCT is one of the highest-resolution imaging modalities that is currently available for in vivo imaging, it cannot capture pores smaller than approximately 100 μm in diameter.[37] However, larger pores, which have the greatest impact on mechanical properties and fragility fracture risk, are resolved.[52] Second, our sample size was relatively small. Increasing the sample size could further confirm or improve the findings of our study. Third, the focus of this study was to investigate the longitudinal changes in cortical porosity in patients undergoing RYGB surgery; therefore, it did not include a control group. Because only patients undergoing RYGB surgery were included, the results of this study are not generalizable to sleeve gastrectomy or other types of bariatric surgery. Finally, because users of bone-active medications were excluded from this cohort, interactions between such medications and pore development remain to be investigated.

Despite these limitations, the findings of this study may have potential clinical implications. We found that longitudinal increases in cortical porosity were on average the greatest in postmenopausal women and that the majority of these increases occurred in the midcortical and periosteal layers. These findings are insightful because they suggest that mechanisms other than trabecularization—for example, expansion of the vascular network in the cortex—may be responsible for driving the increase in cortical porosity. A better understanding of these mechanisms may result in developing more targeted therapeutics to prevent bone loss and, ideally, reduce fracture risk in patients undergoing gastric bypass surgery.

Acknowledgments

The authors thank bariatric surgeons Drs Lygia Stewart, Stanley Rogers, Jonathan Carter, and Andrew Posselt. Funding provided by Department of Veterans Affairs (5 IK2 CX000549); National Center for Advancing Translational Sciences, National Institutes of Health (NIH),through UCSF-CTSI grant UL1 TR000004; National Institute of Diabetes, Digestive, and Kidney Diseases, NIH (R01 DK107629, R21 DK112126, and P30DK098722); UCSF Core Center for Musculoskeletal Biology in Medicine, National Institute of Arthritis and Musculoskeletal and Skin Diseases, NIH (P30 AR075055); National Institute of Arthritis and Musculoskeletal and Skin Diseases (NIAMS), NIH (R03 AR064004); and National Institute of Arthritis and Musculoskeletal and Skin Diseases (NIAMS), NIH (R01 AR069670).

Data Availability Statement

The data that support the findings of this study are available on request from the corresponding author. The data are not publicly available due to privacy or ethical restrictions.

References

1. Must A, Spadano J, Coakley EH, Field AE, Colditz G, Dietz WH. The disease burden associated with overweight and obesity. JAMA. 1999;282(16):1523–1529. [PubMed: 10546691]
2. Ma C, Avenell A, Bolland M, et al. Effects of weight loss interventions for adults who are obese on mortality, cardiovascular disease, and cancer: systematic review and meta-analysis. BMJ. 2017;359:j4849. [PubMed: 29138133]
3. National Task Force on the Prevention and Treatment of Obesity, National Institutes of Health. Very low-calorie diets. JAMA. 1993;270(8):967–974. [PubMed: 8345648]

4. Wilding JPH, Batterham RL, Calanna S, et al. Once-weekly semaglutide in adults with overweight or obesity. N Engl J Med. 2021;384(11):989–1002. [PubMed: 33567185]
5. Buchwald H, Avidor Y, Braunwald E, et al. Bariatric surgery: a systematic review and meta-analysis. JAMA. 2004;292(14):1724–1738. [PubMed: 15479938]
6. Christou NV, Sampalis JS, Liberman M, et al. Surgery decreases long-term mortality, morbidity, and health care use in morbidly obese patients. Ann Surg. 2004;240(3):416–424. [PubMed: 15319713]
7. Lindeman KG, Greenblatt LB, Rourke C, Bouxsein ML, Finkelstein JS, Yu EW. Longitudinal 5-year evaluation of bone density and microarchitecture after Roux-en-Y gastric bypass surgery. J Clin Endocrinol Metab. 2018;103(11):4104–4112. [PubMed: 30219833]
8. Mahdy T, Atia S, Farid M, Adulatif A. Effect of Roux-en Y gastric bypass on bone metabolism in patients with morbid obesity: Mansoura experiences. Obes Surg. 2008;18(12):1526–1531. [PubMed: 18716852]
9. Yu EW, Bouxsein ML, Putman MS, et al. Two-year changes in bone density after Roux-en-Y gastric bypass surgery. J Clin Endocrinol Metab. 2015;100(4):1452–1459. [PubMed: 25646793]
10. Coates PS, Fernstrom JD, Fernstrom MH, Schauer PR, Greenspan SL. Gastric bypass surgery for morbid obesity leads to an increase in bone turnover and a decrease in bone mass. J Clin Endocrinol Metab. 2004;89(3):1061–1065. [PubMed: 15001587]
11. Fleischer J, Stein EM, Bessler M, et al. The decline in hip bone density after gastric bypass surgery is associated with extent of weight loss. J Clin Endocrinol Metab. 2008;93(10):3735–3740. [PubMed: 18647809]
12. Gagnon C, Schafer AL. Bone health after bariatric surgery. JBMR Plus. 2018;2(3):121–133. [PubMed: 30283897]
13. Yu EW. Bone metabolism after bariatric surgery. J Bone Miner Res. 2014;29(7):1507–1518. [PubMed: 24677277]
14. Lu CW, Chang YK, Chang HH, et al. Fracture risk after bariatric surgery: a 12-year nationwide cohort study. Medicine (Baltimore). 2015;94(48):1–7.
15. Yu EW, Kim SC, Sturgeon DJ, Lindeman KG, Weissman JS. Fracture risk after Roux-en-Y gastric bypass vs adjustable gastric banding among Medicare beneficiaries. JAMA Surg. 2019;154(8):746–753. [PubMed: 31090893]
16. Nakamura KM, Haglind EGC, Clowes JA, et al. Fracture risk following bariatric surgery: a population-based study. Osteoporos Int. 2014;25(1):151–158. [PubMed: 23912559]
17. Axelsson KF, Werling M, Eliasson B, et al. Fracture risk after gastric bypass surgery: a retrospective cohort study. J Bone Miner Res. 2018;33(12):2122–2131. [PubMed: 30011091]
18. Fashandi AZ, Mehaffey JH, Hawkins RB, Schirmer B, Hallowell PT. Bariatric surgery increases risk of bone fracture. Surg Endosc. 2018;32(6):2650–2655. [PubMed: 29713829]
19. Rousseau C, Jean S, Gamache P, et al. Change in fracture risk and fracture pattern after bariatric surgery: nested case–control study. BMJ. 2016;354:1–12.
20. Paccou J, Martignène N, Lespessailles E, et al. Gastric bypass but not sleeve gastrectomy increases risk of major osteoporotic fracture: French population-based cohort study. J Bone Miner Res. 2020;35(8):1415–1423. [PubMed: 32187759]
21. Ahmed LA, Shigdel R, Joakimsen RM, et al. Measurement of cortical porosity of the proximal femur improves identification of women with nonvertebral fragility fractures. Osteoporos Int. 2015;26(8):2137–2146. [PubMed: 25876879]
22. Bala Y, Zebaze R, Ghasem-Zadeh A, et al. Cortical porosity identifies women with osteopenia at increased risk for forearm fractures. J Bone Miner Res. 2014;29(6):1356–1362. [PubMed: 24519558]
23. Patsch JM, Burghardt AJ, Yap SP, et al. Increased cortical porosity in type 2 diabetic postmenopausal women with fragility fractures. J Bone Miner Res. 2013;28(2):313–324. [PubMed: 22991256]
24. Bjørnerem Å. The clinical contribution of cortical porosity to fragility fractures. Bonekey Rep. 2016;5(April):1–5.
25. Schafer AL, Kazakia GJ, Vittinghoff E, et al. Effects of gastric bypass surgery on bone mass and microarchitecture occur early and particularly impact postmenopausal women. J Bone Miner Res. 2018;33(6):975–986. [PubMed: 29281126]

26. Burr DB, Hirano T, Turner CH, Hotchkiss C, Brommage R, Hock JM. Intermittently administered human parathyroid hormone(1-34) treatment increases intracortical bone turnover and porosity without reducing bone strength in the humerus of ovariectomized cynomolgus monkeys. J Bone Miner Res. 2001;16(1):157–165. [PubMed: 11149480]
27. Burr DB. Cortical bone: a target for fracture prevention? Lancet. 2010;375(9727):1672–1673. [PubMed: 20472154]
28. Hacker-Thompson A, Robertson TP, Sellmeyer DE. Validation of two food frequency questionnaires for dietary calcium assessment. J Am Diet Assoc. 2009;109(7):1237–1240. [PubMed: 19559142]
29. Lang TF, Li J, Harris ST, Genant HK. Assessment of vertebral bone mineral density using volumetric quantitative CT. J Comput Assist Tomogr. 1999;23(1):130–137. [PubMed: 10050823]
30. Engelke K, Mastmeyer A, Bousson V, Fuerst T, Laredo JD, Kalender WA. Reanalysis precision of 3D quantitative computed tomography (QCT) of the spine. Bone. 2009;44(4):566–572. [PubMed: 19070691]
31. Khosla S, Riggs BL, Atkinson EJ, et al. Effects of sex and age on bone microstructure at the ultradistal radius: a population-based noninvasive in vivo assessment. J Bone Miner Res. 2006;21(1):124–131. [PubMed: 16355281]
32. Boutroy S, Bouxsein ML, Munoz F, Delmas PD. In vivo assessment of trabecular bone microarchitecture by high-resolution peripheral quantitative computed tomography. J Clin Endocrinol Metab. 2005;90(12):6508–6515. [PubMed: 16189253]
33. Bonaretti S, Vilayphiou N, Chan CM, et al. Operator variability in scan positioning is a major component of HR-pQCT precision error and is reduced by standardized training. Osteoporos Int. 2017;28(1):245–257. [PubMed: 27475931]
34. Pialat JB, Burghardt AJ, Sode M, Link TM, Majumdar S. Visual grading of motion induced image degradation in high resolution peripheral computed tomography: impact of image quality on measures of bone density and micro-architecture. Bone. 2012;50(1):111–118. [PubMed: 22019605]
35. Burghardt AJ, Buie HR, Laib A, Majumdar S, Boyd SK. Reproducibility of direct quantitative measures of cortical bone microarchitecture of the distal radius and tibia by HR-pQCT. Bone. 2010;47(3):519–528. [PubMed: 20561906]
36. Tjong W, Kazakia GJ, Burghardt AJ, Majumdar S. The effect of voxel size on high-resolution peripheral computed tomography measurements of trabecular and cortical bone microstructure. Med Phys. 2012;39(4):1893–1903. [PubMed: 22482611]
37. Nirody JA, Cheng KP, Parrish RM, et al. Spatial distribution of intracortical porosity varies across age and sex. Bone. 2015;75:88–95. [PubMed: 25701139]
38. Tjong W, Nirody J, Burghardt AJ, Carballido-Gamio J, Kazakia GJ. Structural analysis of cortical porosity applied to HR-pQCT data. Med Phys. 2014;41(1):1–12. [PubMed: 28519896]
39. Nishiyama KK, Pauchard Y, Nikkel LE, et al. Longitudinal HR-pQCT and image registration detects endocortical bone loss in kidney transplantation patients. J Bone Miner Res. 2015;30(3):456–463.
40. Tjong W, Burghardt AJ, Patsch JM, Majumdar S, Kazakia GJ.The effect of image registration and endocortical segmentation methods on longitudinal HR-pQCT analysis of cortical bone quality. Minneapolis, MN: American Society for Bone and Mineral Research; 2012. Available from:. http://repositorio.unan.edu.ni/2986/1/5624.pdf.
41. Block G, Woods M, Potosky A, Clifford C. Validation of a self-administered diet history questionnaire using multiple diet records. J Clin Epidemiol. 1990;43(12):1327–1335. [PubMed: 2254769]
42. Kim Y, Park I, Kang M. Convergent validity of the International Physical Activity Questionnaire (IPAQ): meta-analysis. Public Health Nutr. 2013;16(3):440–452. [PubMed: 22874087]
43. Kazakia GJ, Tjong W, Nirody JA, et al. The influence of disuse on bone microstructure and mechanics assessed by HR-pQCT. Bone. 2014;63:132–140. [PubMed: 24603002]
44. Tjong W, Nirody J, Carballido-Gamio J, et al. Longitudinal analysis of cortical pore structure using HR-pQCT W. Minneapolis, MN: American Society for Bone and Mineral Research; 2012. Available from:. http://repositorio.unan.edu.ni/2986/1/5624.pdf.

45. Heilmeier U, Cheng K, Pasco C, et al. Cortical bone laminar analysis reveals increased midcortical and periosteal porosity in type 2 diabetic postmenopausal women with history of fragility fractures compared to fracture-free diabetics. Osteoporos Int. 2016;27(9):2791–2802. [PubMed: 27154435]

46. Trueta J. Blood supply and the rate of healing of tibial fractures. Clin Orthop Relat Res. 1974;105:11–26.

47. Ringelstein EB, Dittrich R, Stögbauer F. Borderzone infarcts. In Caplan LR, van Gijn J, eds. Stroke syndromes. 3rd ed. Cambidge, UK: Cambridge University Press; 2012 pp 480–500.

48. Turnbull TL, Baumann AP, Roeder RK. Fatigue microcracks that - initiate fracture are located near elevated intracortical porosity but not elevated mineralization. J Biomech. 2014;47(12):3135–3142. [PubMed: 25065731]

49. Loundagin LL, Pohl AJ, Edwards WB. Stressed volume estimated by finite element analysis predicts the fatigue life of human cortical bone: the role of vascular canals as stress concentrators. Bone. 2021;143:115647. [PubMed: 32956853]

50. Whiting WC, Zernicke RF. Biomechanics of musculoskeletal injury. 2nd ed. Champaign, IL: Human Kinetics; 2008.

51. Zebaze RM, Ghasem-Zadeh A, Bohte A, et al. Intracortical remodelling and porosity in the distal radius and post-mortem femurs of women: a cross-sectional study. Lancet. 2010;375(9727):1729–1736. [PubMed: 20472174]

52. Zimmermann EA, Schaible E, Bale H, et al. Age-related changes in the plasticity and toughness of human cortical bone at multiple length scales. Proc Natl Acad Sci U S A. 2011;108(35):14416–14421. [PubMed: 21873221]

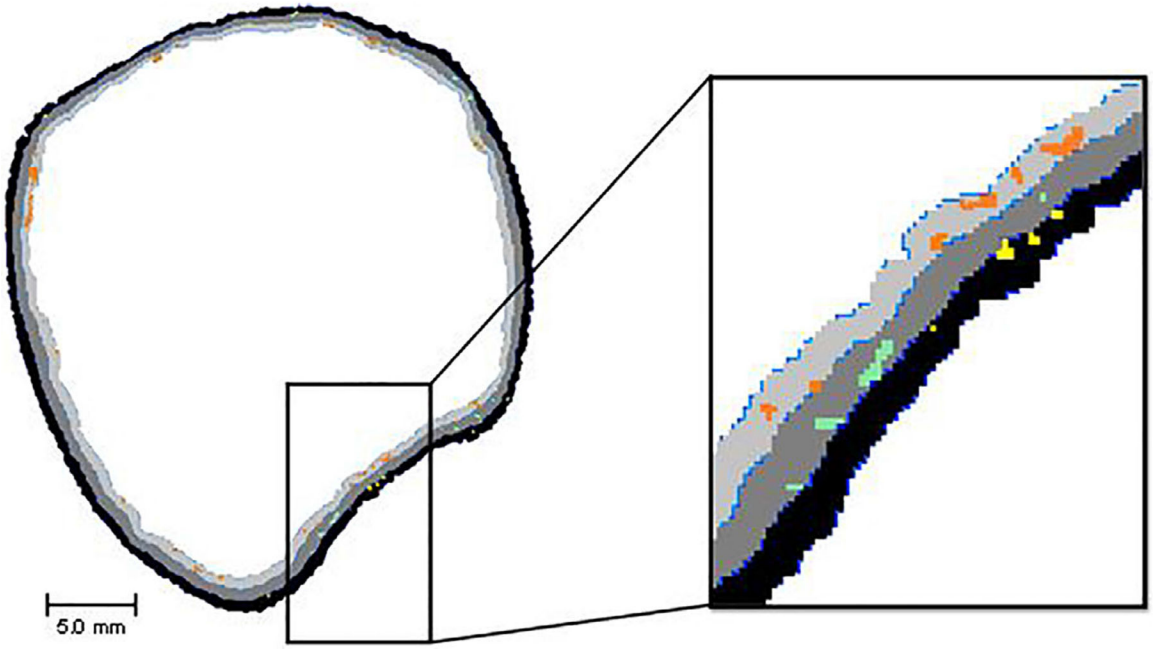

Fig. 1.

A representative cortical pore laminar mask for a distal tibia scan, delineating the pores within the three cortical layers. Pores classified as endosteal are shown in orange, pores classified as midcortical are shown in green, and pores classified as periosteal are shown in yellow.

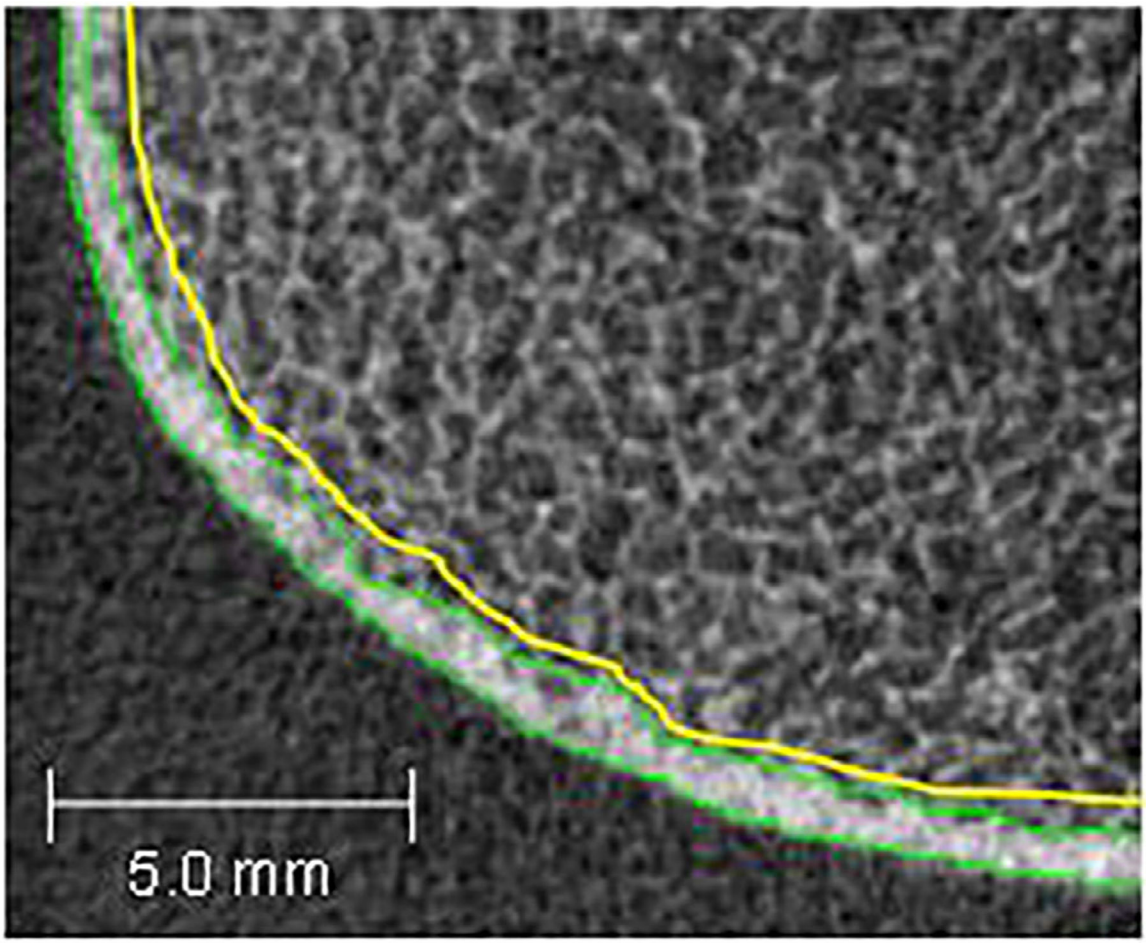

Fig. 2.

A representative baseline-mapped endosteal boundary definition shown for a quadrant of one distal tibia. The green contour is the standard endosteal boundary for the follow-up data set; the yellow contour is the endosteal boundary using the baseline-mapping technique (a schematic emphasizing the difference for better illustration).

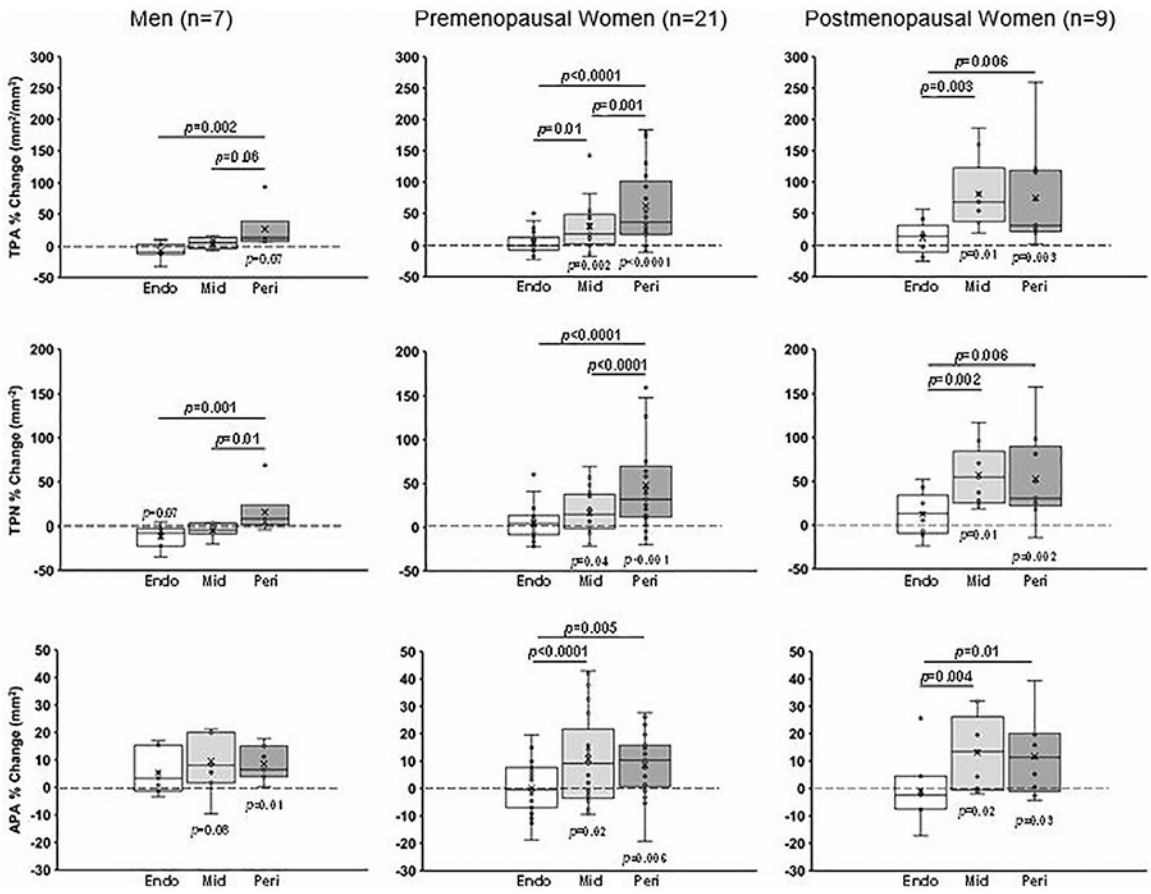

Fig. 3.

Sex- and menopause-specific percent changes (from baseline to 12-month follow-up) in total pore area (TPA, mm^2/mm^2), total pore number (TPN, mm^{-2}), and average pore area (APA, mm^2) at the distal tibia, shown in each laminar layer (Endo = endosteal layer; Mid = midcortical layer; Peri = periosteal layer). The *p* values on horizontal bars are between layers; *p* values below or above boxes are between baseline and follow-up. Mixed models were used for between-layer comparisons. Paired *t* tests were used to compare baseline versus follow-up measurements in each layer.

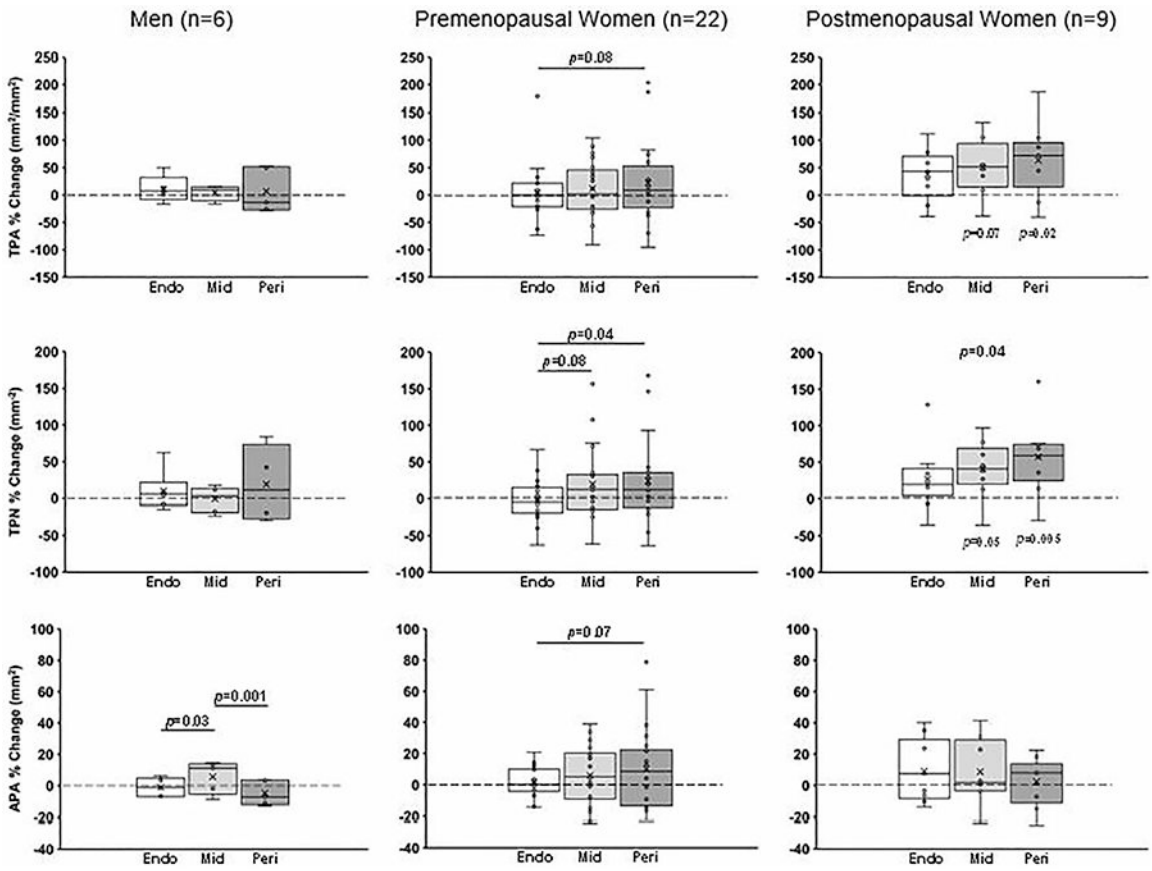

Fig. 4.

Sex- and menopause-specific percent changes (from baseline to 12-month follow-up) in total pore area (TPA, mm^2/mm^2), total pore number (TPN, mm^{-2}), and average pore area (APA, mm^2) at the distal radius, shown in each laminar layer (Endo = endosteal layer; Mid = midcortical layer; Peri = periosteal layer). The *p* values on horizontal bars are between layers; *p* values below or above boxes are between baseline and follow-up. Mixed models were used for between-layer comparisons. Paired *t* tests were used to compare baseline versus follow-up measurements in each layer.

Table 1.

Baseline Characteristics, Stratified by Sex and Menopause Status

Characteristic	All participants (*n* = 42)	Men (*n* = 9)	Premenopausal women *n* = 23)	Postmenopausal women (*n* = 10)
Age (years)	46 ± 12	52 ± 13	39 ± 8[a]	54 ± 8[b]
Race, *n*				
White	25 (60%)	7 (78%)	11 (48%)	7 (70%)
Black	8 (19%)	0 (0%)	6 (26%)	2 (20%)
Asian	2 (5%)	1 (11%)	1 (4%)	0 (0%)
Native Hawaiian/Pacific Islander	2 (5%)	1 (11%)	1 (4%)	0 (0%)
Hispanic/Latino	5 (12%)	0 (0%)	4 (17%)	1 (10%)
Diabetes, *n*	16 (38%)	7 (78%)	4 (17%)	5 (50%)
Weight (kg)	121 ± 18	134 ± 16	121 ± 17	110 ± 17[a]
Body mass index (kg/m^2)	44 ± 7	41 ± 4	45 ± 8	43 ± 6
Laboratory parameters				
HbA_{1c} (%)	5.6 (5.3, 6.6)	6.6 (6.0, 9.6)	5.4 (5.1, 5.8)[a]	6.3 (5.6, 7.0)[b]
25(OH)D upon enrollment (ng/mL)	24 (17, 29)	27 (22, 38)	21 (17, 26)	23 (17, 34)
PTH (pg/mL)	42 (34, 55)	41 (34, 63)	43 (36, 54)	47 (27, 66)
Cholesterol (mg/dL)	165 (136, 195)	127 (108, 178)	175 (150, 219)[a]	173 (153, 192)
Triglyceride (mg/dL)	114 (90, 150)	139 (92, 151)	113 (86, 158)	110 (99, 146)
Lifestyle parameters				
Physical activity (met-min/week)	990 (17, 2744)	906 (50, 4565)	1548 (332, 2730)	308 (0, 2136)
Dietary protein (g/d)	80 ± 31	83 ± 35	83 ± 32	73 ± 26
Dietary protein (% of total kcal)	17 ± 2	17 ± 2	17 ± 3	17 ± 2
Areal BMD (DXA) (g/cm^2)				
Femoral neck	0.944 ± 0.124	0.931 ± 0.081	0.987 ± 0.117	0.857 ± 0.131[b]
Total hip	1.123 ± 0.134	1.148 ± 0.084	1.145 ± 0.159	1.048 ± 0.078
Lumbar spine	1.161 ± 0.138	1.226 ± 0.181	1.166 ± 0.109	1.091 ± 0.136
Areal BMD (DXA) *T-/Z*-scores				
Femoral neck				

Characteristic	All participants (n = 42)	Men (n = 9)	Premenopausal women n = 23)	Postmenopausal women (n = 10)
T-score	0.5 ± 1.0	0.0 ± 0.6	0.9 ± 0.9[a]	−0.2 ± 0.9[b]
Z-score	1.1 ± 0.8	0.8 ± 0.6	1.2 ± 0.9	0.9 ± 0.8
Total hip				
T-score	1.1 ± 1.0	0.8 ± 0.6	1.4 ± 1.1	0.7 ± 0.6
Z-score	1.5 ± 0.9	1.1 ± 0.6	1.6 ± 1.1	1.4 ± 0.6
Lumbar spine				
T-score	0.8 ± 1.2	1.2 ± 1.7	0.9 ± 1.0	0.2 ± 1.2
Z-score	1.3 ± 1.3	1.7 ± 1.8	1.2 ± 1.1	1.3 ± 1.4
Volumetric BMD (QCT) (g/cm^3)				
Spine	0.159 ± 0.038	0.148 ± 0.020	0.177 ± 0.034	0.130 ± 0.037[b]

PTH = parathyroid hormone; BMD = bone mineral density; DXA = dual-energy X-ray absorptiometry; QCT = quantitative computed tomography. Values are shown as means ± SDs, counts (percentages), or medians (interquartile range).

[a] $p < 0.05$ versus men.

[b] $p < 0.05$ versus premenopausal women.

Table 2.

Baseline and Follow-up Values and Relative (%) and Absolute Change in Laminar Analysis Results After Gastric Bypass Surgery at the Distal Tibia (All Participants Pooled, $n = 37$)

Parameter	Baseline	12-month follow-up	Relative change (%)	Absolute change	*p* Value
TPA (mm^2/mm^2)					
Endosteal	0.054 ± 0.021	0.056 ± 0.023	3.80 ± 20.12	0.002 ± 0.010	0.31
Midcortical	0.043 ± 0.031 *	0.055 ± 0.038	37.82 ± 47.16 **	0.010 ± 0.011 **	**0.0001**
Periosteal	0.026 ± 0.019 **##	0.036 ± 0.022 **##	58.77 ± 64.55 **#	0.010 ± 0.009 **	**<0.0001**
TPN (mm^{-2})					
Endosteal	1.234 ± 0.402	1.259 ± 0.413	3.72 ± 21.16	0.025 ± 0.217	0.49
Midcortical	0.927 ± 0.607 **	1.069 ± 0.654 *	22.44 ± 33.02 *	0.108 ± 0.193 *	**0.004**
Periosteal	0.642 ± 0.412 **##	0.843 ± 0.452 **#	43.78 ± 49.59 **#	0.201 ± 0.195 **#	**<0.0001**
APA (mm^2)					
Endosteal	0.043 ± 0.005	0.043 ± 0.005	0.90 ± 10.08	0.0002 ± 0.005	0.84
Midcortical	0.047 ± 0.013 *	0.051 ± 0.013 **	11.08 ± 15.03 **	0.004 ± 0.007 **	**0.0002**
Periosteal	0.038 ± 0.006 *##	0.041 ± 0.007 ##	9.33 ± 11.10 **	0.003 ± 0.004 *	**<0.0001**

TPA = total pore area (sum of all pore areas in each layer divided by the area of that layer, averaged over all slices [mm^2/mm^2]); TPN = total pore number (total number of pores in each layer, divided by the area of that layer, averaged over all slices [mm^{-2}]); APA = average pore area (mean pore area in each layer [mm^2]).

* $p < 0.05$

** $p < 0.0001$ versus the endosteal, and

\# $p < 0.05$

\#\# $p < 0.0001$ versus the midcortical layer; *p* value represents comparison between baseline and follow-up.

Table 3.

Baseline and Follow-up Values and Relative (%) and Absolute Change in Laminar Analysis Results After Gastric Bypass Surgery at the Distal Radius (All Participants Pooled, $n = 37$)

Parameter	Baseline	12-month follow-up	Relative change (%)	Absolute change	*p* Value
TPA (mm^2/mm^2)					
Endosteal	0.021 ± 0.011	0.023 ± 0.014	13.37 ± 47.11	0.0001 ± 0.006	0.35
Midcortical	0.018 ± 0.011	0.021 ± 0.017	20.31 ± 49.87	0.003 ± 0.010 *	0.07
Periosteal	0.009 ± 0.008 **##	0.010 ± 0.009 **##	30.68 ± 69.27 *	0.003 ± 0.006	0.21
TPN (mm^{-2})					
Endosteal	0.584 ± 0.290	0.620 ± 0.299	7.64 ± 34.84	−0.002 ± 0.169	0.35
Midcortical	0.439 ± 0.293 **	0.509 ± 0.343 *	21.28 ± 44.01	0.055 ± 0.166 *	**0.03**
Periosteal	0.171 ± 0.101 **##	0.230 ± 0.160 **##	32.24 ± 55.60 *	0.059 ± 0.109 *	**0.003**
APA (mm^2)					
Endosteal	0.035 ± 0.005	0.036 ± 0.006	2.89 ± 12.59	0.001 ± 0.005	0.24
Midcortical	0.043 ± 0.010 **	0.045 ± 0.009 **	6.53 ± 17.77	0.002 ± 0.008	0.14
Periosteal	0.038 ± 0.009 *#	0.040 ± 0.011 *#	6.07 ± 22.16	0.002 ± 0.008	0.17

TPA = total pore area (sum of all pore areas in each layer divided by the area of that layer, averaged over all slices [mm^2/mm^2]); TPN = total pore number (total number of pores in each layer, divided by the area of that layer, averaged over all slices [mm^{-2}]); APA = average pore area (mean pore area in each layer [mm^2]).

* $p < 0.05$

** $p < 0.0001$ versus the endosteal, and***

\# $p < 0.05$

\#\# $p < 0.0001$ versus the midcortical layer; p value represents comparison between baseline and follow-up.

Table 4.

Longitudinal Changes in Porosity Parameters Calculated Using Standard and Baseline Mapping Techniques at the Distal Tibia (All Participants Pooled, $n = 37$)

Parameter	Relative change without baseline mapping (%)	Relative change with baseline mapping (%)	*p* Value
Ct.Th	−3.41 ± 4.42	−0.45 ± 3.47	**0.0002**
Ct.Po.V	16.95 ± 26.39	18.62 ± 28.38	0.59
Ct.Po	16.05 ± 18.01	18.79 ± 29.67	0.41
Po.Dm	6.06 ± 8.71	6.18 ± 7.61	0.86
Po.Dm.SD	6.99 ± 13.76	7.93 ± 12.88	0.56

Ct.Th = cortical thickness (mm); Ct.Po.V = cortical pore volume (mm^3); Ct.Po = cortical porosity (unitless ratio); Po.Dm = mean cortical pore diameter (mm); Po.Dm.SD = SD of mean cortical pore diameter (mm).

The *p* value represents difference between relative change calculations.

Table 5.

Longitudinal Changes in Porosity Parameters Calculated Using Standard and Baseline Mapping Techniques at the Distal Radius (All Participants Pooled, $n = 37$)

Parameter	Relative change without baseline mapping (%)	Relative change with baseline mapping (%)	*p* Value
Ct.Th	−2.94 ± 4.53	1.17 ± 6.22	**0.002**
Ct.Po.V	10.32 ± 32.64	14.84 ± 32.54	0.10
Ct.Po	12.88 ± 32.52	18.09 ± 40.72	0.48
Po.Dm	3.87 ± 9.77	6.15 ± 9.67	0.13
Po.Dm.SD	5.00 ± 19.79	11.63 ± 22.34	0.08

Ct.Th = cortical thickness (mm); Ct.Po.V = cortical pore volume (mm^3); Ct.Po = cortical porosity (unitless ratio); Po.Dm = mean cortical pore diameter (mm); Po.Dm.SD = SD of mean cortical pore diameter (mm).

The *p* value represents difference between relative change calculations.